25-hydroxycholesterol Regulates Migration, Invasion and EMT of Colorectal Cancer through miR-92a-3p/ACAA1/NF-κB Pathway

Saisai Wang
The First Affiliated Hospital of zhejiang university
Rushan Fei
the affiliated hospital of zhejiang university
Xijuan Xu
the first affiliated hospital of zhejiang university
Jie Xu
the first affiliated hospital of zhejiang university
Yuanyuan Yao
the first affiliated hospital of zhejiang university
Jiying Lu
the first affliated hospital of zhejiang university
Gang Zheng
the 2nd affliated hospital of zhejiang university
Sen Lu
the first affiliated hospital of zhejiang university
wenbin chen (wenbinchen@zju.edu.cn)
First Hospital of Zhejiang Province: Zhejiang University School of Medicine First Affiliated Hospital

Research Article

Keywords: 25-hydroxycholesterol, colorectal cancer, EMT, migration, miR-92a-3p, ACAA1

Posted Date: June 7th, 2021

DOI: https://doi.org/10.21203/rs.3.rs-480136/v1

Abstract

Background: Colorectal cancer (CRC) is one of the most common malignances worldwide. Several studies suggest a positive association between high plasma cholesterol level and CRC. 25-hydroxycholesterol (25-HC) is enzymatically produced by cholesterol 25-hydorxylase in various organs and is involved in many processes. However, the critical role of 25-HC in the tumor growth and progression of CRC is largely unknown.

Methods: CCK-8 assay, flow cytometry and Transwell migration and invasion assays were used to determine the effects of 25-HC on CRC cells proliferation, apoptosis and metastasis. Subcutaneous xenograft model and intra-splenic injection mouse model were established to investigate the effects of 25-HC on CRC *in vivo*. Immunohistochemistry staining was performed to determine the matrix metalloproteinases (MMPs) expressions in mice tumors and acetyl-CoA acyltransferase 1 (ACAA1) expression in human CRC tissues. The expressions of E-cadherin, N-cadherin and Vimentin were examined by immunofluorescent staining. MiR-92a-3p mimic, inhibitor and ACAA1 vector were constructed and transfected into LoVo cells.

Results: 25-HC promotes CRC cells migration, invasion, and metastasis both *in vitro* and *in vivo* without affecting cells proliferation and apoptosis, accompanied by the upregulation of the expressions of MMPs and epithelial-mesenchymal transition (EMT) related markers. Mechanistically, miR-92a-3p expression is significantly elevated after 25-HC stimulation, while ACAA1 expression is down-regulated and negatively associated with tumor progression. Luciferase reporter assay confirms that miR-92a-3p could directly target ACAA1. Subsequent investigation indicates that nuclear factor (NF)-κB signaling is the downstream pathways of miR-92a-3p-ACAA1 axis in CRC cells.

Conclusions: 25-HC promotes CRC cells metastasis by regulating cells migration, invasion and EMT through miR-92a-3p/ACAA1/NF-κB pathway.

Trial registration: The current study was approved by the Ethics Committee of the First Affiliated Hospital, Zhejiang University on March22, 2018. The permission number was 2018-706 and 2020-1000.

Background

Colorectal cancer (CRC) remains one of the most common malignancies worldwide(1). Despite improvements in early screening, diagnosis, surgical techniques and multidisciplinary approaches, the prognosis of CRC patients remains unsatisfactory(2). The leading cause of cancer deaths is distant metastasis and recurrence which greatly hinders the successful treatment(3). Diet is one of the major factors that exert a majorly influence on CRC risk. Among them, cholesterol has a positive association with CRC progression(4). Cholesterol metabolism is involved in the regulation of various tumor biological processes, especially oncogenic signaling pathways, ferroptosis, and tumor microenvironment(5). In breast, prostate and pancreatic cancer, cholesterol has been reported to play the pro-cancerous and pro-proliferative role(6, 7). Targeting cholesterol metabolism as a new therapeutic approach has received increasing attention. Therefore, the relationship between cholesterol and CRC needs further exploration.

25-hydroxycholesterol (25-HC), one form of oxysterol, is enzymatically produced by cholesterol 25-hydorxylase (Ch25h) in various organs including lung, kidney and heart(8, 9). 25-HC plays multiple roles in lipid metabolism, antivirus process, inflammatory response and cell survival (10). The antiviral effect of 25-HC has been widely investigated in murine norovirus(11), Zika virus(12), SARS-CoV-2(13), herpes simplex-1 virus(14) and so on. Recently, the role of 25-HC in cancer has gradually attracted researchers' attentions. Chen *et al.* reported 25-HC promotes the lung adenocarcinoma cells migration and invasion in an LXR (liver X receptor)-dependent manner(15). In human bladder cancer cells, 25-HC promotes proliferation, epithelial-to-mesenchymal transition (EMT) and adriamycin

resistance in T24 and RT4 cells. Moreover, high levels of 25-HC in bladder cancer are associated with a poor outcome(16). Our previous study also found 25-HC decreases the sensitivity of human gastric cancer cells to 5-fluorouracil and promotes cells invasion *via* the TLR2/NF-κB signaling pathway(17) and promotes hepatocellular carcinoma metastasis through up-regulation of TLR4 dependent FABP4(18). Conversely, in head and neck squamous cell carcinoma, 25-HC-could induce cells apoptosis which is dependent on the activation of caspases by Fas antigen ligand-triggered death receptor-mediated extrinsic pathway and mitochondria-dependent intrinsic pathway *via* mitogen activated protein kinases(19).

Cancer-related inflammation is recognized as a tumor hallmark(20). Increasing evidence indicates that chronic inflammation has wide-ranging effects on CRC pathogenesis. The effect of 25-HC on inflammation is controversial. Activation of macrophages lacking Ch25h expression leads to overproduction of inflammatory interleukin-1 family cytokines, indicating the anti-inflammatory effects of 25-HC(21). 25-HC also reduces lipopolysaccharide (LPS)-induced TNF-α expression and secretion in macrophages(22). In contrast, 25-HC enhances LPS-induced IL-1β secretion in apo4-expressing microglia(23) and IL-6 production in macrophages(24). In response to obesogenic stimuli, 25-HC exerts a promotive role in the progression of meta-inflammation and insulin resistance in obese humans and mouse models of obesity(25). Moreover, 25-HC has been reported to contribute to cerebral inflammation of X-linked adrenoleukodystrophy through activation of the NLRP3 inflammasome(26). Based on these findings, we hypothesis that 25-HC might be involved in the progression and development of CRC.

In the present study, we demonstrated for the first time that 25-HC promoted CRC migration, invasion and EMT both *in vitro* and *in vivo*, without affecting cell proliferation and apoptosis. MiR-92a-3p up-regulation and the targeted ACAA1 down-regulation was critical for the promotive function of 25-HC. Additionally, ACAA1 was down-regulated in CRC tissues and inhibited CRC cells migration and invasion. Lastly, we revealed the promotion of CRC cells invasion was, at least partly due to the activation of NF-κB signaling. These results suggested that 25-HC promoted CRC cell migration, invasion and EMT through miR-92a-3p/ACAA1/NF-κB pathway.

Methods

Cell lines and reagents

Human CRC cell lines (LoVo, SW480 and SW620) and normal mucosal epithelial cell line NCM460 were purchased from American Type Culture Collection (ATCC, Manassas, VA, USA). All cell lines were cultured in RPMI-1640 containing 10% FBS in a humidified incubator at 37℃ with 5% CO_2. All cell culture reagents were purchased from Invitrogen (Shanghai, China).

25-HC was purchased from Sigma-Aldrich (Shanghai, China) and dissolved in ethanol as a stock solution. Human recombinant ACAA1 was bought from Abcam (Shanghai, China).

Cell viability assay

Cell viability was determined by CCK-8 assay. Briefly, cells were plated at 1×10^4 cells/well in 96-well plates and incubated for 24 hours in RPMI-1640 complete medium before treated with 25-HC at 2.5, 5 and 10 μM. The cell proliferation was measured after culturing for another 24, 48 and 72 hours using a Cell Counting Kit-8 (Dojindo, Japan) according to the manufacturer's instructions. Absorbance was measured at a wavelength of 450 nm.

Cell apoptosis assay

CRC cells treated with the indicated concentrations of 25-HC for 48 hours before cells were harvested and stained with the Annexin V apoptosis kit (Lianke Biotech, Co., Ltd.) according to the manufacturer's instructions. The stained cells were then subjected to flow cytometry analysis using a BD FACScan system (BD Biosciences, San Jose, CA, USA).

Protein isolation and Western blotting analysis

Antibodies used for Western blotting were as follows: rabbit anti-Bcl-2 monoclonal antibody (mAb, #4223, CST, Danvers, MA, USA), rabbit anti-caspase-3 Ab (#9662, CST), rabbit anti-caspase-6 Ab (#9762, CST), rabbit anti-β-actin mAb (#8457, CST), rabbit anti-MMP1 polyclonal antibody (pAb, #10371-2-AP, Proteintech, Wuhan, China)), rabbit anti-MMP2 pAb (#10373-2-AP, Proteintech), rabbit anti-MMP3 pAb (#17873-1-AP, Proteintech), rabbit anti-MMP9 pAb (#10375-2-AP, Proteintech), rabbit anti-MMP13 pAb (#18165-1-AP, Proteintech), rabbit anti-ACAA1 pAb (#12319-2-AP, Proteintech), rabbit anti-Snail pAb (#13099-1-AP, Proteintech), rabbit anti-E-cadherin mAb (#3195, CST), rabbit anti-N-cadherin mAb (#13116, CST), rabbit anti-Vimentin pAb (ab137321, Abcam, USA), mouse anti-GAPDH (#60004-1-Ig, Proteintech). Briefly, protein was isolated from cells with 1× RIPA buffer containing 1 mM phenylmethylsulfonyl fluoride (PMSF) (CST) and protease inhibitor cocktail. Thirty to fifty micrograms of total proteins were run on a 10% polyacrylamide gel, and then transferred to polyvinylidene difluoride membranes. After blocking, membranes were incubated overnight at 4°C with the primary antibodies followed with the secondary HRP-conjugated anti-mouse or anti-rabbit antibodies. β-actin or GAPDH was used as an internal control. Densitometric analysis was performed with Image J software. The density for each band was normalized to that of GAPDH. The relative expression of each protein was compared to the control, which was assigned a value of 1.

Xenograft mouse model and *in vivo* metastasis mouse model

The animal study was approved by the Animal Care and Use Committee of Zhejiang University. 5-6-week-old female Balb/C nude mice were purchased from Shanghai Laboratory Animal Company (SLAC; Shanghai, China) and maintained in the animal facility at Zhejiang University.

For xenograft mouse model, mice were divided into two groups (PBS and 25-HC group) and subcutaneously injected with 1×10^6 LoVo cells. Mice in 25-HC group received 25-HC (10 mg/kg) *via* intraperitoneal injection every 3 days for 3 weeks. Mice in control group received the equal volume of PBS. The maximum diameter (a) and minimum diameter (b) of tumor were measured with a vernier caliper every 3 days after tumor formation. Tumor volumes were calculated by the formula: $(a \times b^2)/2$. Finally, all the mice were sacrificed, and the xenograft was collected.

For *in vivo* metastasis mouse model, LoVo cells (2×10^6) in 100 μL ice-cold PBS were injected into the spleen of the anesthetized mice before the spleen was returned to the abdomen and the wound was sutured with 5-0 black silk. Mice in 25-HC group received 25-HC (10 mg/kg) *via* intraperitoneal injection every 3 days for 3 weeks. Mice in control group received the equal volume of PBS. Twenty days later, mice were sacrificed. Spleens and livers were removed and observed. The number of the metastasis foci formation in the livers were counted and then processed for H&E or IHC staining. H&E and IHC staining were performed by Servicebio Company (Wuhan, China).

In vitro migration and invasion assays

Cell migration and invasion assays were performed with the 8 μm Transwell chambers (Corning Costar, NY, USA). Briefly, 200 μL of LoVo cells at a density of 2×10^5/mL were resuspended in culture medium containing 2% FBS and different concentrations of 25-HC were added to the upper chamber, whereas 600 μL medium supplemented with 20% FBS was added to the lower chamber. After incubation for 36 hours, cells were fixed with ice-cold methanol and

stained with 0.5% crystal violet. The stained cells were observed and counted under a microscope. For invasion assay, the upper chamber was pre-coated with 1 mg/mL Matrigel (BD Biosciences).

Immunohistochemistry staining

Immunohistochemistry staining (IHC) was performed by Servicebio Company (Wuhan, China). Briefly, formalin-fixed, paraffin-embedded sections were prepared from livers of the nude mice or human CRC tissues and its adjacent non-tumor tissues. IHC staining of mouse livers were performed with MMP1, MMP3 and MMP9 antibodies and IHC staining of the human tissues were performed with ACAA1 antibody. The immunostaining of CRC sections was reviewed by two investigators (SSW and RSF) in a blinded manner and graded into ACAA1-high-expression group (> 30% of tumor cells were positively stained) and ACAA1-low-expression group (< 30% of tumor cells were positively stained).

Tissue samples

Eight pairs of human CRC tissues and corresponding normal tissues were obtained for IHC from January 2013 to October 2013.Twenty pairs of fresh human colorectal cancer tissues, corresponding peri-tumor and normal tissues were obtained for RT-qPCR or Western blotting from May 2018 to August 2018. All the tissues were collected from the First Affiliated Hospital, Zhejiang University School of Medicine (Hangzhou, China) and from the patients who had not received any chemotherapy or radiotherapy before surgery. Clinical data including age, gender, tumor location, TNM stage, distant metastasis, tumor size and CEA level were collected from medical records. The experimental protocol was approved by the Human Experimental Ethical Inspection of the First Affiliated Hospital and the informed consent of patients was acquired. Eight patients in this work have been followed up until death or to five years after surgery.

Immunofluorescent staining

LoVo cells seeded on coverslips were treated with the indicated concentrations of 25-HC for 24 hours before fixed with 4% paraformaldehyde for 10 min and permeabilized with 0.1% (v/v) Triton X-100 for 5 min at room temperature. The cells were then incubated overnight with primary antibodies against E-cadherin, N-cadherin and Vimentin at 4°C, followed by incubation with FITC-conjugated secondary antibody for 2 hour at room temperature. Cells were then stained with fluorochrome dye DAPI (Sigma-Aldrich) to visualize the nucleus. Images were examined and captured using a laser scanning confocal microscope (Olympus Fluoview FV1000, Japan) with a peak excitation wave length of 570 nm and 340 nm.

RNA Extraction and qRT-PCR Analysis

Total RNA of cells or tissues was extracted with Ultrapure RNA Kit (CW Biotech, Beijing, China). Then the RNA was converted to cDNA by iScript cDNA synthesis kit (Bio-Rad) or miRNA cDNA Synthesis kit (Cwbiotech, Beijing, China) according to the manufacturer's instructions. Quantitative real-time PCR analysis of E-cadherin, N-cadherin, Vimentin, ACAA1, MMP1, MMP2, and MMP9 were performed with the iTaq Universal SYBR Green Supermix (Bio-Rad) and the miR-92a-3p expression level was determined with miRNA qPCR Assay Kit (Cwbiotech). Relative expression levels were calculated by $2^{-\Delta\Delta CT}$ method. Primers used for qRT-PCR are listed in Table 1.

Cell transfection

MiR-92a-3p mimic, miR-92a-3p inhibitor and its relative negative control (NC) were synthesized by GenePharma (Shanghai, China). The sequences are as follows (28): miR-92a-3p mimic: 3'-UGUCCGGCCCUGUUCACGUUAU-5',

miR-92a-3p inhibitor: 3'-ACAGGCCGGGACAAGUG CAAUA-5', miR-92a-3p mimic NC: 5'-UUUGUACUACACAAAAGUACUG-3', miR-92a-3p inhibitor NC: 5'-CAGUACUUUUGUGUAGUACAAA-3'. Full length clone DNA of human ACAA1 was bought from Vigene Biosciences (Shandong, China). Transfections were carried out with the Lipofectamine 2000 transfection reagent (Invitrogen) according to the manufacturer's instructions.

Luciferase reporter assay

Wild-type (Wt) or the mutated type (Mut) of ACAA1-3'-UTR containing miR-92a-3p binding sites was synthesized by GenePharma (Shanghai, China) and cloned downstream of the luciferase reporter gene. LoVo cells were seeded into 96-well plates (1×10^4 cells/well) one day before and then co-transfected with the Wt ACAA1-3'-UTR or the Mut ACAA1-3'-UTR vectors (500 ng) and the miR-92a-3p mimics or negative controls with Lipofectamine 2000 transfection reagent. After 48 hours of transfection, cells were harvested, and the luciferase activity was detected with the dual-luciferase reporter assay system (Promega, Madison, WI, USA).

To detect the NF-κB activation, LoVo cells were transiently transfected with NF-κB luciferase reporter plasmid or co-transfected with miR-92a-3p inhibitor or ACAA1 over-expression plasmid with Lipofectamine 2000 transfection reagent. After 24 hours post transfection, cells were stimulated with 25-HC for the indicated concentrations. After 24 hours, cells were harvested, and the luciferase activities were determined by using the Bright-Glo luciferase assay system (Promega).

Bioinformatics analysis

Oncomine database (http://www.oncomine.org) was selected to search the ACAA1 expression levels between CRC and normal groups. The TargetScan prediction tool (www.targetscan.org) and PicTar (http://pictar.mdc-berlin.de/) were used to predict genes binding to the miR-92a-3p.

Statistical analysis

Data are expressed as means ± SEM. and analyzed by GraphPad Prism 6. Statistical significance was determined by Student's *t*-test or one-way analysis of variance (ANOVA) followed by Dunnett's test. The relationship between ACAA1 expression and the CRC clinical features was analyzed with the Chi-square test. *p*-value <0.05 was considered as statistical significance.

Results

25-HC has no effects on CRC cells proliferation and apoptosis

In order to examine the role of 25-HC in CRC, we first detected the cells proliferation of NCM460 and three human CRC cell lines treated with 25-HC by CCK-8 assay. As shown in Figure 1A, 2.5-10 μM of 25-HC had no effects on cells proliferation. Subsequently, the impact of 25-HC on CRC cells apoptosis and expressions of apoptosis-related proteins were examined by flow cytometry (Figure 1B) and Western blotting (Figure 1C), respectively. Consistently, 25-HC had no impact on cells apoptosis. To investigate the role of 25-HC in tumorigenesis *in vivo*, we injected LoVo cells into nude mice followed by treatment with 25-HC. In consistent with the *in vitro* results, the tumor size and weight had no significant differences treated with or without 25-HC (Figure 1D). These results suggest that 25-HC has no effects on CRC cells proliferation and apoptosis.

25-HC promotes CRC cells migration and invasion both *in vitro* and *in vivo*

Next, transwell assay was performed to determine the effects of 25-HC on LoVo cells migration and invasion. Interestingly, 25-HC treatment significantly increased the number of LoVo cells migrating and invading through the transwell membrane (Figure 2A). Consistently, the expressions of MMPs including MMP1, 2, 3, 9 and 13 were significantly enhanced in a dose- and time-dependent manner (Figure 2B).

By construction of the spleen-liver metastasis model, we detected the role of 25-HC in CRC metastasis *in vivo*. As shown in Figure 3A, 25-HC remarkably enhanced metastatic potential of LoVo cells as evidenced by the significantly increased metastasis nodules in the liver (20±2.2 *vs* 4.3±1.3, p=0.0008). Furthermore, IHC staining results showed the expressions of MMP1, MMP3 and MMP9 in the metastasis nodules in the liver after 25-HC treatment were dramatically higher than that without 25-HC stimulation (Figure 3B). Taken together, these results provide important insights that 25-HC played a promotive role in the migration and invasion of CRC cells both *in vitro* and *in vivo*.

25-HC regulates EMT of CRC cells

Epithelial-to-mesenchymal transition (EMT) plays an essential role in the migration and invasion of tumor cells. Therefore, the EMT-related markers were detected by Western blotting analysis in LoVo cells. As shown in Figure 4A, 25-HC significantly decreased the expression of epithelial marker E-cadherin, while increased the expressions of mesenchymal markers N-cadherin, Vimentin and Snail. The result of immunofluorescence assay further displayed that 25-HC up-regulated N-cadherin and Vimentin expression while down-regulated E-cadherin expression (Figure 4B). The mRNA level and protein level of E-cadherin, N-cadherin and Vimentin in xenografts from the nude mice were also detected by RT-qPCR and Western blotting, respectively. As shown in Figure 4C and 4D, in line with the *in vitro* results, 25-HC up-regulated N-cadherin and Vimentin expressions accompanying with down-regulated E-cadherin expression. Overall, these results suggest that 25-HC promotes CRC cells migration and invasion possibly by regulating EMT.

The effects of 25-HC on CRC cells migration and EMT is mediated by up-regulation of miR-92a-3p

Considering that miRNAs play an important role in cancer, we then explored if specific miRNAs are involved in the 25-HC-promoted CRC cells migration and invasion. We found that the expression of miR-92a-3p was significantly elevated in CRC cells after 25-HC treatment in a dose-dependent manner compared with no-25-HC stimulation (Figure 5A). Subsequently, the role of miR-92a-3p in the pro-tumor effects of 25-HC was further investigated. Interestingly, LoVo cells transfected with miR-92a-3p inhibitor showed reduced cell migration as compared to those transfected with a negative control (miR-NC) (Figure 5B). Meanwhile, miR-29a-3p inhibitor reversed the 25-HC-induced EMT (Figure5C). Additionally, the expressions of MMP1, MMP2, MMP3, MMP9, MMP13, N-cadherin and Vimentin which up-regulated by 25-HC could be partly reversed by miR-92a-3p inhibitor (Figure 5D). These results suggest that 25-HC promotes CRC cells metastasis by inducing cells migration, invasion and EMT *via* modulation of miR-92a-3p.

ACAA1 is a direct target of miR-92a-3p

To further clarify the underlying molecular mechanisms in the modulation of cells migration, invasion and EMT of CRC by miR-92a-3p after 25-HC treatment, bioinformatics predictions (TargetScan and PicTar) were used to identify the potential targets of miR-92a-3p. Among the potential target genes, ACAA1 aroused our attention. Therefore, the expression level of ACAA1 after 25-HC stimulation in LoVo, SW620 and SW480 cells were detected. Strikingly, 25-HC treatment significantly decreased the ACAA1 expression (Figure 6A). Furthermore, transfection of miR-9a-3p mimic dramatically decreased the ACAA1 expression in LoVo cells (Figure 6B). The predicted interaction between miR-92a-3p and the target sites in the ACAA1 3′-UTR was illustrated in Figure 6C. Dual luciferase reporter assay showed that transfection of miR-92a-3p mimic decreased the relative luciferase activity of LoVo cells transfected with Wt ACAA1 3′-UTR but not the Mut ACAA1 3′-UTR. These data suggest that ACAA1 is a direct target of miR-92a-3p. Moreover,

miR-92a-3p inhibitor reversed the down-regulation of ACAA1 induced by 25-HC (Figure 6D). In summary, all these data suggest that miR-92a-3p-ACAA1 axis might be involved in the 25-HC-induced promotive effects in CRC.

Over-expression of ACAA1 reverses the 25-HC-induced migration and EMT in CRC cells

To further investigate the role of ACAA1 in CRC, LoVo cells were either transfected with ACAA1 plasmid or stimulated with ACCA1 reagent. As shown in Figure 7A and 7B, over-expression of ACAA1 and treatment with ACCA1 decreased the mRNA and protein levels of MMP1, MMP2, MMP9, MMP13, N-cadherin and Vimentin, while increased the expression of E-cadherin. Consistently, the migratory capability of LoVo cells were also decreased transfected with ACAA1 or treated with ACAA1 reagent.

Furthermore, the ACAA1 function under 25-HC treatment was explored. Over-expression of ACAA1 reversed the expression level of 25-HC induced MMPs and the EMT markers (Figure 8A) accompanied with the induced LoVo cells migration (Figure 8B) and EMT (Figure 8C). Thus, our current results suggest that the promotive role of 25-HC in CRC migration and EMT was partly mediated by down-regulation of ACAA1.

ACAA1 is down-regulated in CRC and negatively associated with tumor progression

Next, the expression pattern of ACAA1 in human CRC tissues was explored. First, we analyzed the expression levels of ACAA1 RNA between CRC and normal tissues from Oncomine Database and ACAA1 was significantly down-regulated in tumor tissues ($p<0.001$) (Figure 9A). We also collected 20 cases of human CRC tissues, peri-tumor tissues and the corresponding adjacent normal tissues to determine the ACAA1 expression by RT-qPCR and Western blotting, respectively (Figure 9B). ACAA1 was significantly down-regulated in tumor tissues compared with the normal tissues ($p=0.021$). While, the expression of miR-92a-3p was increased in the CRC tissues (Figure 9C). Moreover, analysis the relationship between ACAA1 and miR-92a-3p suggests that their expression was inversely associated with each other (R=-0.7331, $p<0.001$). ACAA1 expression was further examined by IHC in 80 cases of CRC tissues. As illustrated in Figure 9D, ACAA1 was mainly detected in cytoplasm. ACAA1 was less detectable in tumor tissues than in normal tissues and pronounced decreased in tissues from CRC patients with liver metastasis. The correlation between ACAA1 expression and clinicopathological variables of CRC patients was shown in Table 2. Results showed that high levels of ACAA1 was negatively associated with tumor N stage ($p=0.04$), M stage ($p=0.03$) and serum level of CEA ($p=0.036$). No relationship was found between ACAA1 expression and age ($p=0.52$), gender ($p=0.96$), tumor size ($p=0.34$), T stage ($p=0.54$) or tumor location ($p=0.87$). What's more, a striking difference in 5-year survival was observed between the high ACAA1 expression group and the low ACAA1 expression group of CRC patients ($p=0.033$) (Figure 9E).

The promotive migration of 25-HC on CRC cells is mediated by NF-κB activation

To identify which signaling pathways were related to the 25-HC-induced promotive effects, activation of various signaling was performed on LoVo cells by Western blotting analysis. Results demonstrated that 25-HC up-regulated the phosphorylation of NF-κB p65 and PI3K-AKT in a dose- and time-dependent manner, while it decreased the phosphorylation of STAT3 (Figure 10A and 10B). Thus, Bay 11-7082 and Ly294002 were introduced to inhibit the NF-κB p65 and PI3K p85/p55 activation, respectively and the expressions of MMPs and cells migration were determined. Interestingly, inhibition of NF-κB p65 reversed 25-HC-induced cells migration and up-regulated MMP1, MMP9 and MMP13 expressions (Figure 10C and 10D), while inhibition of PI3K p85/p55 had no effects. These results showed that the promotive effects of 25-HC on CRC cells migration was mediated by NF-κB activation.

We then detected the phosphorylation of NF-κB by Western blotting after cells transfected with miR-92a-3p inhibitor or ACAA1 over-expression plasmid. As shown in Figure 11A and 11B, under 25-HC treatment, silencing of miR-92a-3p or over-expression of ACAA1 could down-regulate the phosphorylation of NF-κB accompanying with the NF-κB luciferase units. Taken together, these results suggest that 25-HC regulates migration, invasion and EMT of colorectal cancer through miR-92a-3p/ACAA1/NF-κB pathway.

Discussion

The development and progression of colorectal cancer (CRC) is usually slow but can ultimately lead to metastasis which is the main cause of death. Therefore, various studies have been performed to systematically understand how cancer metastasis occurs and thus, preventing or inhibiting CRC progression(27, 28). In this study, we verified that 25-hydroxycholesterol (25-HC), one form of oxysterol, promotes CRC metastasis by regulating cells migration, invasion and EMT. Mechanistically, we revealed that 25-HC increased the expression of miR-92a-3p while decreased the expression of ACAA1. The interaction between miR-92a-3p and ACAA1 was further confirmed by the luciferase reporter assay.

MiR-92a-3p is a member of highly conserved gene cluster miR-17-92 which is located on 13q31.3. The miR-17-92 cluster, also named as human oncomiR-1, includes miR-17, miR-18a, miR-19a, miR-20a, miR-19b-1 and miR-92a and has been identified to be over-expressed in various cancers(29-31). The roles of miR-92a-3p in cancers have been extensively investigated. In renal cell carcinoma, miR-92a-3p expression level is significantly upregulated and promotes cell proliferation by targeting FBXW7(32). In gastric cancer (GC), the expression of miR-92a-3p is associated with tumor size, lymph node infiltration and distant metastasis, acting as an independent prognostic factor of poor survival in patients with GC. MiR-92a-3p promotes GC cell proliferation, DNA synthesis and invasion by targeting KLF2(33). Moreover, miR-92a-3p promotes proliferation and metastatic potential of glioma cells and inhibits the stemness of glioma stem-like cells by regulating cadherin 1 (CDH1)/β-catenin signaling and Notch-1/Akt signaling, respectively(34). While in Wilms' tumor, miR-92a-3p is significantly downregulated, and inhibits proliferation, migration, invasion, and induces apoptosis of WT cells by targeting FRS2(35) and NOTCH1(36). These studies demonstrate that the exact biological role of miR-92a-3p varies in different cancers.

In CRC, circulating exosomal miR-92a-3p is associated with pathologic stages and grades of the CRC patients(37). Inhibition of miR-92a-3p by locked nucleic acid (LNA) could inhibit cell proliferation and induce apoptosis and necrosis in CRC(38). MiR-92a-3p acts as an oncomiR *via* regulating the phosphatase and tensin homolog deleted on chromosome 10 (PTEN)-mediated PI3K/AKT pathway(39). PTEN is characterized as a lipid and protein phosphatase which is capable of dephosphorylating phospho-peptides as well as phospho-lipids. The lipid phosphatase activity of PTEN is critical for its tumor suppressor function(40). Thus, it is reasonable to reveal that the promotive of 25-HC in CRC is mediated by miR-92a-3p.

Acetyl-CoA acyltransferase 1 (ACAA1) is an enzyme involved in lipid β-oxidation and provides substrates to the tricarboxylic acid (TCA) cycle, a critical step in cellular metabolism. The expression of ACAA1 is significantly down-regulated in 15 types of cancers including CRC. Higher ACAA1 expression level correlates with the higher survival(41). The mechanisms of ACAA1 in cancers are involved in several immune-related process including phagocytosis, regulation of adaptive immune response, regulation of lymphocyte mediated immunity and ECM affiliated(42). Consistently, in our study, RT-qPCR and Western blotting analysis results supported that ACAA1 was down-regulated in CRC tissues. IHC staining data showed that high expression level of ACAA1 was positively correlated with a good prognosis. However, the detailed mechanisms of ACAA1 involved is not sure which needs to be further investigated.

After confirming that miR-92a-3p could directly bind with ACAA1, we further identified which signaling pathway was involved. Results showed that NF-κB phosphorylation was increased by 25-HC and inhibition of miR-92a-3p or over-expression of ACAA1 decreased the 25-HC-induced NF-κB activation, indicating that NF-κB is the down-stream signaling in the 25-HC-miR-92a-3p-ACAA1 induced CRC promotion, though the specific inflammatory molecules were not determined. One study reported that in liposarcoma, miR-92a-3p stimulates secretion of proinflammatory cytokine IL-6 from tumor-associated macrophages in a TLR7/8-dependent manner, which in turn could promotes liposarcoma cell proliferation, invasion, and metastasis by impacting the surrounding microenvironment(43). Thus, the molecules inducing the invasion, EMT and metastasis of CRC cells after 25-HC treatment could be a focus of the follow-up studies.

Conclusion

In conclusion, the present study demonstrated that 25-HC promotes CRC metastasis by regulating cells migration, invasion and EMT. Moreover, 25-HC increases the expression of miR-92a-3p, which directly targets ACAA1. Furthermore, ACAA1 is down-regulated in CRC and predicts a good prognosis of CRC patients. Notably, NF-κB signaling pathway is responsible for the 25-HC-induced promotive effects on CRC cells. Collectively, we identified the active role of 25-HC/miR-92a-3p/ACAA1/NF-κB axis in the progression of CRC and provide insights into developing therapeutic targets for CRC.

Abbreviations

CRC: colorectal cancer; 25-HC: 25-hydroxycholesterol; miRNA: microRNA; MMP: matrix metalloproteinase; EMT: epithelial-to-mesenchymal transition; ACAA1: acetyl-CoA acyltransferase 1; Ch25h: cholesterol 25-hydorxylase; LXR: liver X receptor; TLR: toll-like receptor; IHC: immunohistochemistry staining; qRT-PCR: real-time quantitative polymerase chain reaction; NC: negative control.

Declarations

Ethics approval and consent to participate

Study protocols were approved by the Ethical Inspection of the First Affiliated Hospital, Zhejiang University School of Medicine and written informed consent was obtained from patients based on the Declaration of Helsinki.

Consent for publication

Not applicable.

Availability of data and materials

The datasets used and/or analyzed during the current study are available from the corresponding author on reasonable request.

Competing interests

The authors declare that they have no competing interests.

Funding

This work was supported by the Key Project of Natural Science Foundation of Zhejiang Province (LZ21H160004 to WC) and National Natural Science Foundation of China (81902408 to SW).

Authors' contributions

SW, RF and WC participated in the conception and design of the study. SW, RF, JX, LY, JL and YY performed the statistical analysis and were involved in the preparation of the figures. SW, JX, LY and JL reviewed the results and participated in the discussion of the data. RF, GZ and WC prepared the manuscript and revised it. All authors read and approved the manuscript and agreed to be accountable for all aspects of the research in ensuring that the accuracy or integrity of any part of the work are appropriately investigated and resolved.

Acknowledgements

Not applicable.

Authors' information

Not applicable.

References

1. Siegel RL, Miller KD, Jemal A. Cancer statistics, 2020. CA Cancer J Clin. 2020;70(1):7-30.
2. van der Valk MJM, Hilling DE, Bastiaannet E, Meershoek-Klein Kranenbarg E, Beets GL, Figueiredo NL, et al. Long-term outcomes of clinical complete responders after neoadjuvant treatment for rectal cancer in the International Watch & Wait Database (IWWD): an international multicentre registry study. Lancet. 2018;391(10139):2537-45.
3. Bhullar DS, Barriuso J, Mullamitha S, Saunders MP, O'Dwyer ST, Aziz O. Biomarker concordance between primary colorectal cancer and its metastases. EBioMedicine. 2019;40:363-74.
4. Azeem S, Gillani SW, Siddiqui A, Jandrajupalli SB, Poh V, Syed Sulaiman SA. Diet and Colorectal Cancer Risk in Asia–a Systematic Review. Asian Pac J Cancer Prev. 2015;16(13):5389-96.
5. Xu H, Zhou S, Tang Q, Xia H, Bi F. Cholesterol metabolism: New functions and therapeutic approaches in cancer. Biochim Biophys Acta Rev Cancer. 2020;1874(1):188394.
6. Llaverias G, Danilo C, Mercier I, Daumer K, Capozza F, Williams TM, et al. Role of cholesterol in the development and progression of breast cancer. Am J Pathol. 2011;178(1):402-12.
7. Jung YY, Ko JH, Um JY, Chinnathambi A, Alharbi SA, Sethi G, et al. LDL cholesterol promotes the proliferation of prostate and pancreatic cancer cells by activating the STAT3 pathway. J Cell Physiol. 2020.
8. Hosseinpour F, Wikvall K. Porcine microsomal vitamin D(3) 25-hydroxylase (CYP2D25). Catalytic properties, tissue distribution, and comparison with human CYP2D6. J Biol Chem. 2000;275(44):34650-5.
9. Blanc M, Hsieh WY, Robertson KA, Kropp KA, Forster T, Shui G, et al. The transcription factor STAT-1 couples macrophage synthesis of 25-hydroxycholesterol to the interferon antiviral response. Immunity. 2013;38(1):106-18.
10. Cao Q, Liu Z, Xiong Y, Zhong Z, Ye Q. Multiple Roles of 25-Hydroxycholesterol in Lipid Metabolism, Antivirus Process, Inflammatory Response, and Cell Survival. Oxid Med Cell Longev. 2020;2020:8893305.
11. Shawli GT, Adeyemi OO, Stonehouse NJ, Herod MR. The Oxysterol 25-Hydroxycholesterol Inhibits Replication of Murine Norovirus. Viruses. 2019;11(2).

12. Li C, Deng YQ, Wang S, Ma F, Aliyari R, Huang XY, et al. 25-Hydroxycholesterol Protects Host against Zika Virus Infection and Its Associated Microcephaly in a Mouse Model. Immunity. 2017;46(3):446-56.
13. Zu S, Deng YQ, Zhou C, Li J, Li L, Chen Q, et al. 25-Hydroxycholesterol is a potent SARS-CoV-2 inhibitor. Cell Res. 2020;30(11):1043-5.
14. Cagno V, Civra A, Rossin D, Calfapietra S, Caccia C, Leoni V, et al. Inhibition of herpes simplex-1 virus replication by 25-hydroxycholesterol and 27-hydroxycholesterol. Redox Biol. 2017;12:522-7.
15. Chen L, Zhang L, Xian G, Lv Y, Lin Y, Wang Y. 25-Hydroxycholesterol promotes migration and invasion of lung adenocarcinoma cells. Biochem Biophys Res Commun. 2017;484(4):857-63.
16. Wang C, He H, Fang W. Oncogenic roles of the cholesterol metabolite 25-hydroxycholesterol in bladder cancer. Oncol Lett. 2020;19(6):3671-6.
17. Wang S, Yao Y, Rao C, Zheng G, Chen W. 25-HC decreases the sensitivity of human gastric cancer cells to 5-fluorouracil and promotes cells invasion via the TLR2/NF-kappaB signaling pathway. Int J Oncol. 2019;54(3):966-80.
18. Wang S, Yao Y, Wang X, Zheng G, Ouyang W, Chen W. 25-HC promotes hepatocellular carcinoma metastasis through up-regulation of TLR4 dependent FABP4. Am J Cancer Res. 2019;9(10):2140-55.
19. You JS, Lim H, Kim TH, Oh JS, Lee GJ, Seo YS, et al. 25-Hydroxycholesterol Induces Death Receptor-mediated Extrinsic and Mitochondria-dependent Intrinsic Apoptosis in Head and Neck Squamous Cell Carcinoma Cells. Anticancer Res. 2020;40(2):779-88.
20. Taniguchi K, Karin M. NF-kappaB, inflammation, immunity and cancer: coming of age. Nat Rev Immunol. 2018;18(5):309-24.
21. Reboldi A, Dang EV, McDonald JG, Liang G, Russell DW, Cyster JG. Inflammation. 25-Hydroxycholesterol suppresses interleukin-1-driven inflammation downstream of type I interferon. Science. 2014;345(6197):679-84.
22. Englund MC, Karlsson AL, Wiklund O, Bondjers G, Ohlsson BG. 25-hydroxycholesterol induces lipopolysaccharide-tolerance and decreases a lipopolysaccharide-induced TNF-alpha secretion in macrophages. Atherosclerosis. 2001;158(1):61-71.
23. Wong MY, Lewis M, Doherty JJ, Shi Y, Cashikar AG, Amelianchik A, et al. 25-Hydroxycholesterol amplifies microglial IL-1beta production in an apoE isoform-dependent manner. J Neuroinflammation. 2020;17(1):192.
24. Gold ES, Diercks AH, Podolsky I, Podyminogin RL, Askovich PS, Treuting PM, et al. 25-Hydroxycholesterol acts as an amplifier of inflammatory signaling. Proc Natl Acad Sci U S A. 2014;111(29):10666-71.
25. Russo L, Muir L, Geletka L, Delproposto J, Baker N, Flesher C, et al. Cholesterol 25-hydroxylase (CH25H) as a promoter of adipose tissue inflammation in obesity and diabetes. Mol Metab. 2020;39:100983.
26. Jang J, Park S, Jin Hur H, Cho HJ, Hwang I, Pyo Kang Y, et al. 25-hydroxycholesterol contributes to cerebral inflammation of X-linked adrenoleukodystrophy through activation of the NLRP3 inflammasome. Nat Commun. 2016;7:13129.
27. Allgayer H, Leupold JH, Patil N. Defining the "Metastasome": Perspectives from the genome and molecular landscape in colorectal cancer for metastasis evolution and clinical consequences. Semin Cancer Biol. 2020;60:1-13.
28. Geng F, Wang Z, Yin H, Yu J, Cao B. Molecular Targeted Drugs and Treatment of Colorectal Cancer: Recent Progress and Future Perspectives. Cancer Biother Radiopharm. 2017;32(5):149-60.
29. Kuo G, Wu CY, Yang HY. MiR-17-92 cluster and immunity. J Formos Med Assoc. 2019;118(1 Pt 1):2-6.

30. Olive V, Jiang I, He L. mir-17-92, a cluster of miRNAs in the midst of the cancer network. Int J Biochem Cell Biol. 2010;42(8):1348-54.
31. Fang LL, Wang XH, Sun BF, Zhang XD, Zhu XH, Yu ZJ, et al. Expression, regulation and mechanism of action of the miR-17-92 cluster in tumor cells (Review). Int J Mol Med. 2017;40(6):1624-30.
32. Zeng R, Huang J, Sun Y, Luo J. Cell proliferation is induced in renal cell carcinoma through miR-92a-3p upregulation by targeting FBXW7. Oncol Lett. 2020;19(4):3258-68.
33. Mao QQ, Chen JJ, Xu WJ, Zhao XZ, Sun X, Zhong L. miR-92a-3p promotes the proliferation and invasion of gastric cancer cells by targeting KLF2. J Biol Regul Homeost Agents. 2020;34(4):1333-41.
34. Song H, Zhang Y, Liu N, Zhao S, Kong Y, Yuan L. miR-92a-3p Exerts Various Effects in Glioma and Glioma Stem-Like Cells Specifically Targeting CDH1/beta-Catenin and Notch-1/Akt Signaling Pathways. Int J Mol Sci. 2016;17(11).
35. Li JL, Luo P. MiR-140-5p and miR-92a-3p suppress the cell proliferation, migration and invasion and promoted apoptosis in Wilms' tumor by targeting FRS2. Eur Rev Med Pharmacol Sci. 2020;24(1):97-108.
36. Zhu S, Zhang L, Zhao Z, Fu W, Fu K, Liu G, et al. MicroRNA92a3p inhibits the cell proliferation, migration and invasion of Wilms tumor by targeting NOTCH1. Oncol Rep. 2018;40(2):571-8.
37. Fu F, Jiang W, Zhou L, Chen Z. Circulating Exosomal miR-17-5p and miR-92a-3p Predict Pathologic Stage and Grade of Colorectal Cancer. Transl Oncol. 2018;11(2):221-32.
38. Ahmadi S, Sharifi M, Salehi R. Locked nucleic acid inhibits miR-92a-3p in human colorectal cancer, induces apoptosis and inhibits cell proliferation. Cancer Gene Ther. 2016;23(7):199-205.
39. Ke TW, Wei PL, Yeh KT, Chen WT, Cheng YW. MiR-92a Promotes Cell Metastasis of Colorectal Cancer Through PTEN-Mediated PI3K/AKT Pathway. Ann Surg Oncol. 2015;22(8):2649-55.
40. Myers MP, Pass I, Batty IH, Van der Kaay J, Stolarov JP, Hemmings BA, et al. The lipid phosphatase activity of PTEN is critical for its tumor supressor function. Proc Natl Acad Sci U S A. 1998;95(23):13513-8.
41. Feng H, Shen W. ACAA1 Is a Predictive Factor of Survival and Is Correlated With T Cell Infiltration in Non-Small Cell Lung Cancer. Front Oncol. 2020;10:564796.
42. Zhang X, Yang H, Zhang J, Gao F, Dai L. HSD17B4, ACAA1, and PXMP4 in Peroxisome Pathway Are Down-Regulated and Have Clinical Significance in Non-small Cell Lung Cancer. Front Genet. 2020;11:273.
43. Casadei L, Calore F, Creighton CJ, Guescini M, Batte K, Iwenofu OH, et al. Exosome-Derived miR-25-3p and miR-92a-3p Stimulate Liposarcoma Progression. Cancer Res. 2017;77(14):3846-56.

Tables

Table 1. Sequences of primers used in the study.

Gene	Forward Primer	Reverse Primer
MMP1	CTCTGGAGTAATGTCACACCTCT	TGTTGGTCCACCTTTCATCTTC
MMP2	CCCACTGCGGTTTTCTCGAAT	CAAAGGGGTATCCATCGCCAT
MMP9	AGACCTGGGCAGATTCCAAAC	CGGCAAGTCTTCCGAGTAGT
E-cadherin	CGAGAGCTACACGTTCACGG	GGGTGTCGAGGGAAAAATAGG
N-cadherin	TCAGGCGTCTGTAGAGGCTT	ATGCACATCCTTCGATAAGACTG
Vimentin	GACGCCATCAACACCGAGTT	CTTTGTCGTTGGTTAGCTGGT
ACAA1	GCGGTTCTCAAGGACGTGAAT	GTCTCCGGGATGTCACTCAGA
β-actin	GTATCCTGACCCTGAAGTACC	TGAAGGTCTCAAACATGATCT
miR-92a-3p	UAUUGCACUGUCCCGGCCUGU	CTCAACTGGTGTCGTGGAGTCGGCAATTCAGTTGAGACAGGCCG
U6	CTCGTTCGGCAGCACA	AACGCTTCACGAATTTGCGT

Table 2. Correlation between ACAA1 levels in CRC patients and their clinicopathological characteristics.

Characteristics	ACAA1 levels		χ2	*p*-value
	Low (n=37)	High (n=43)		
Age (years)			0.41	0.52
<60	19	19		
≥60	18	24		
Gender			0.0026	0.96
Female	17	20		
Male	20	23		
Tumor size (cm)			0.93	0.34
<5	22	30		
≥5	15	13		
T factor			0.27	0.54
T1+T2	19	25		
T3+T4	18	18		
N factor			4.22	**0.04***
N0	13	25		
N1+N2	24	18		
M factor			4.66	**0.03***
M0	17	30		
M1	20	13		
Tumor location			0.025	0.87
rectal	20	22		
colon	17	21		
CEA (ng/ml)			4.393	**0.036***
<5	12	24		
≥5	25	19		

Figures

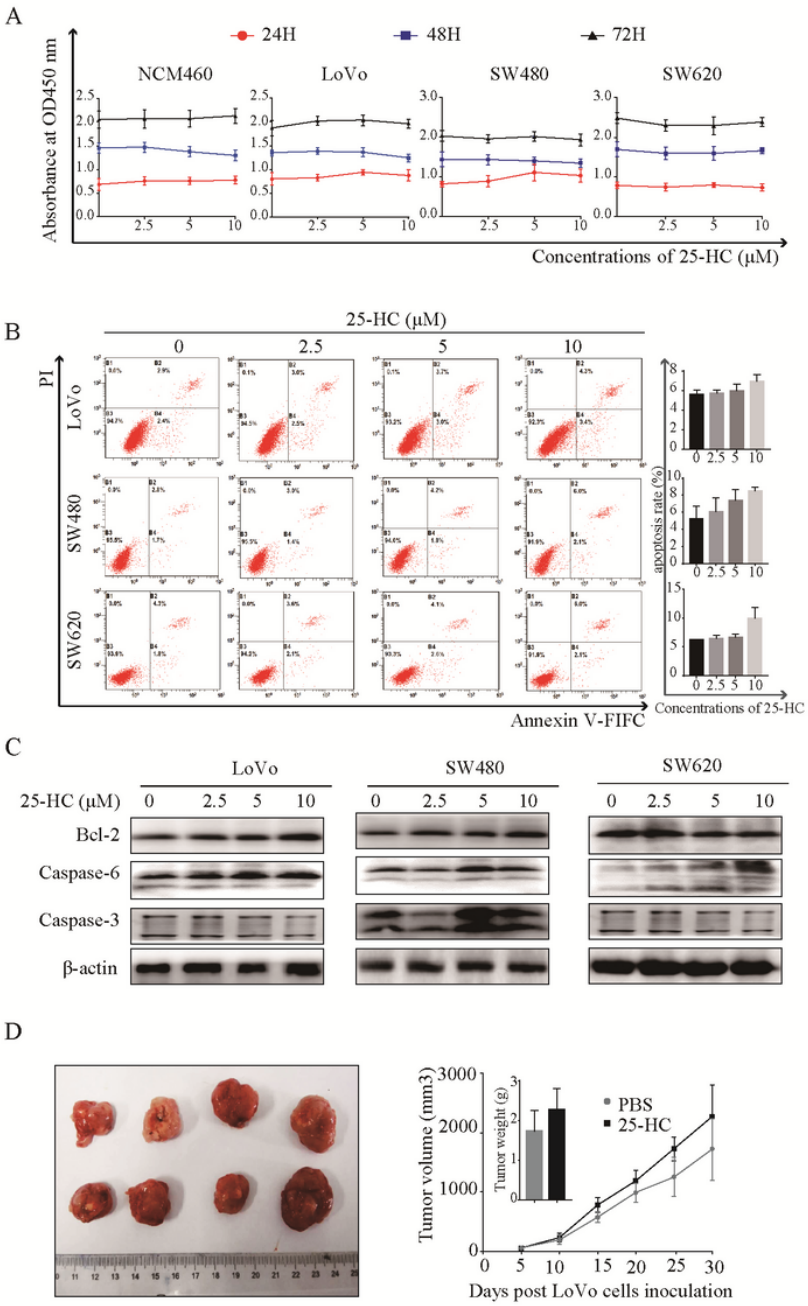

Figure 1

25-HC has no effects on CRC cells proliferation in vitro and in vivo. (A) The cell proliferative ability of NCM460, LoVo, SW480 and SW620 cells were detected by CCK-8 assay after 25-HC treatment for 24, 48 and 72 hours. (B) The apoptosis of LoVo, SW480 and SW620 cells were examined by flow cytometry after 25-HC treatment for 48 hours. (C) The protein level of Bcl-2, Caspase-6 and Caspase-3 were detected by Western blotting after 25-HC treatment for 48 hours. (D) Nude mice were subcutaneously injected with LoVo cells followed by PBS or 25-HC treatment. The volume of the tumor and the body weight was recorded. Results were obtained from 3 independent experiments and are expressed as the means ± SEM.

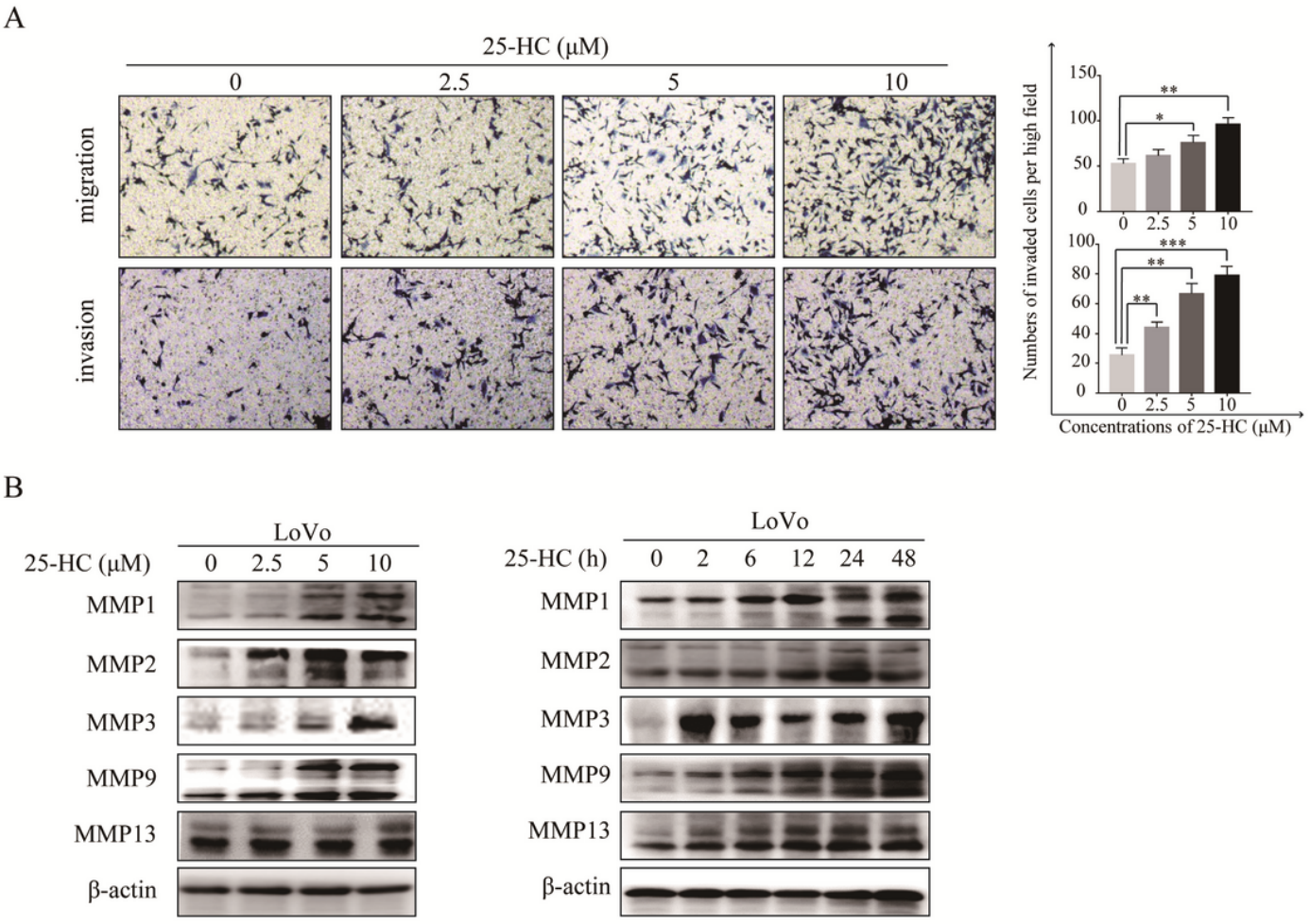

Figure 2

25-HC promotes CRC cells migration and invasion in vitro. LoVo cells were treated with the indicated concentrations of 25-HC for 24 hours, (A) cells migration and invasion were assessed by the Transwell assay. (B) cells were collected and proteins were extracted for Western blotting to determine the MMP1, MMP2, MMP3, MMP9 and MMP13 expressions. Results were obtained from 3 independent experiments and are expressed as the means ± SEM. *p<0.05, **p<0.01, ***p< 0.001.

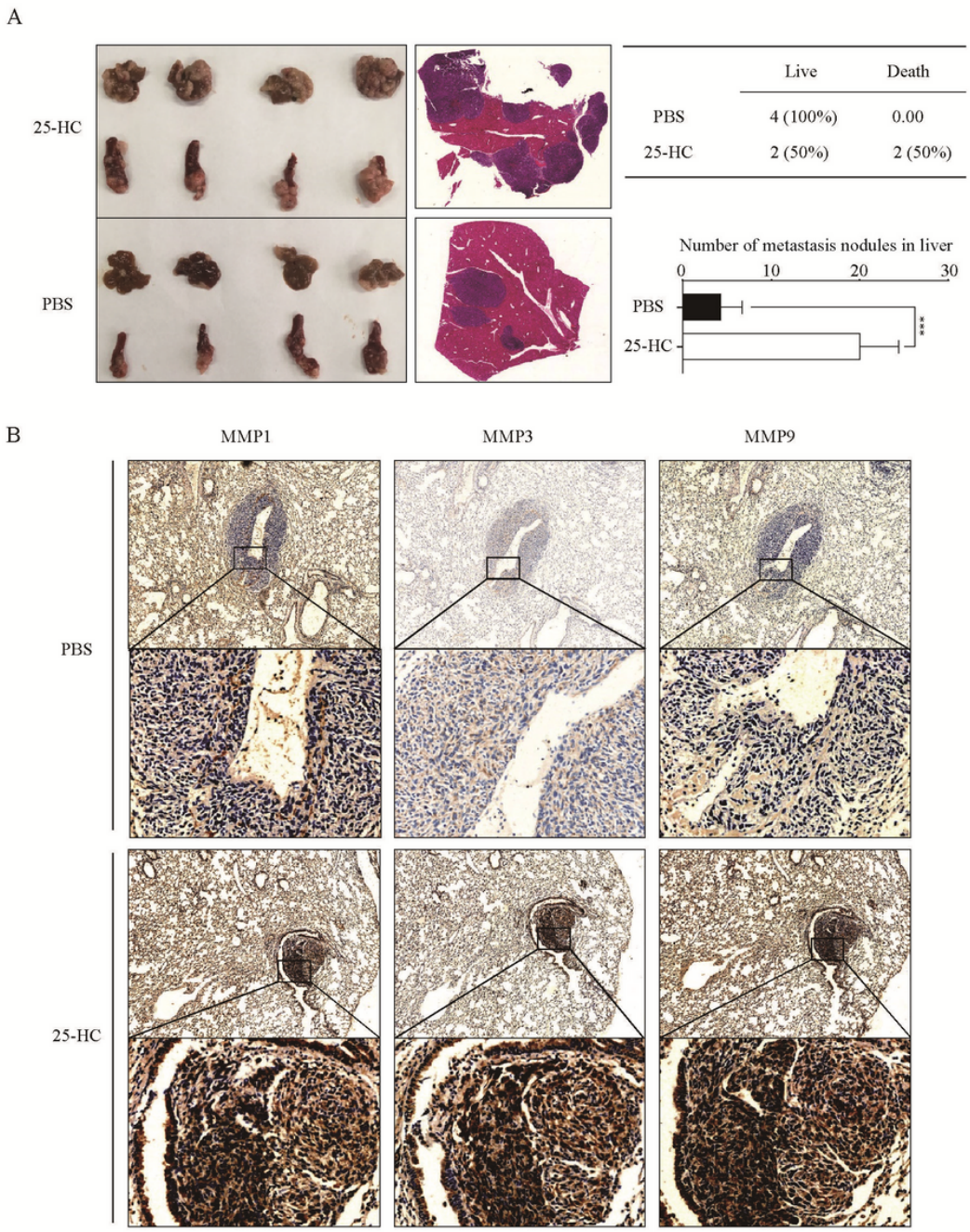

Figure 3

25-HC promotes metastasis of CRC cells in vivo. Nude mice were intrasplenically injected with LoVo cells followed by PBS and 25-HC treatment. At the end of the experiment, liver and spleen were collected. (A) Numbers of metastatic lesions in the liver were counted. Magnification, ×4. (B) Immunohistochemical staining for MMP1, MMP2 and MMP9 in the liver were performed. Magnification, ×100. Results were obtained from 2 independent experiments and are expressed as the means ± SEM. ***p< 0.001.

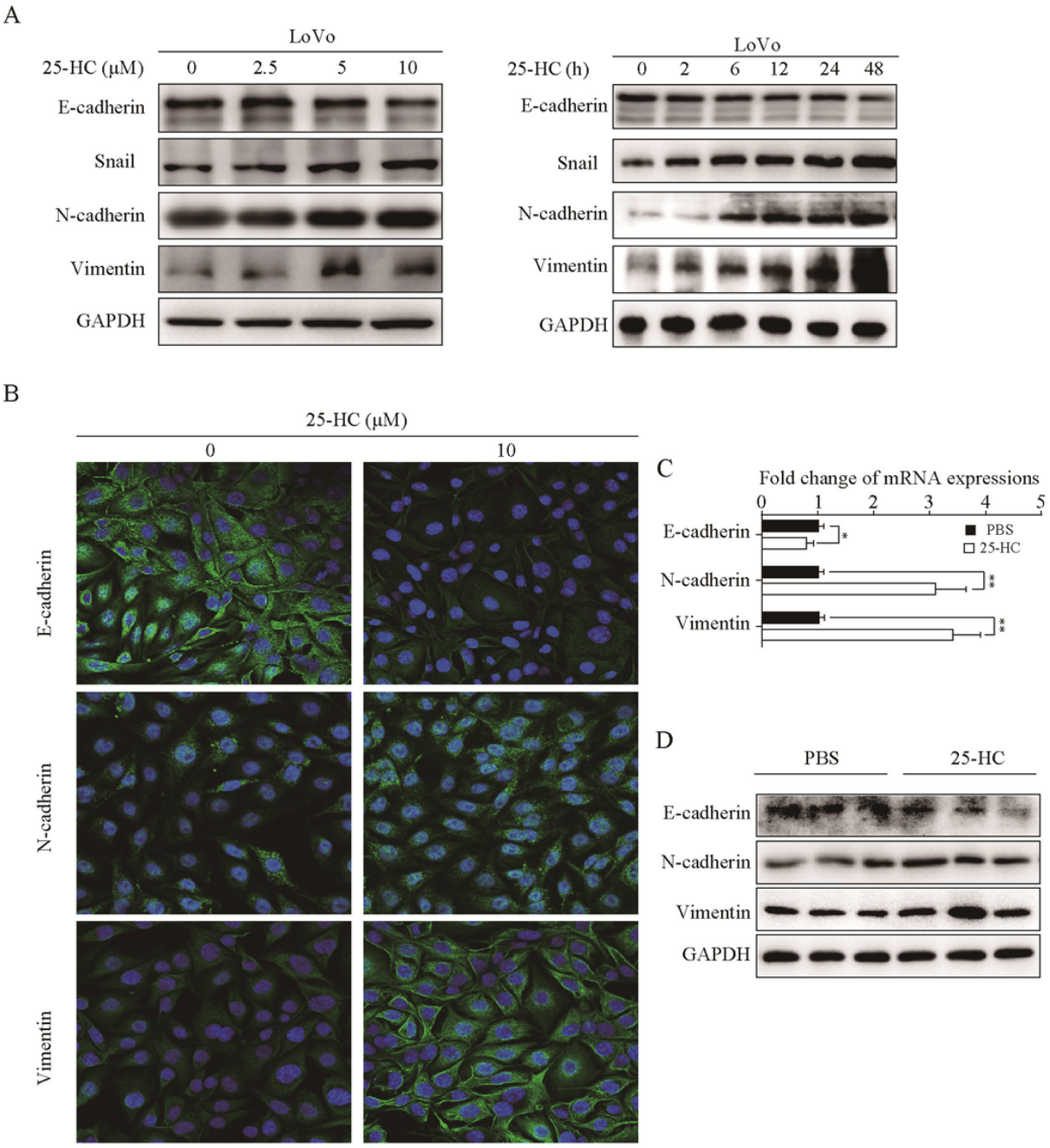

Figure 4

25-HC induces EMT in CRC cells. (A) LoVo cells were stimulated with the indicated concentrations of 25-HC for 24 hours, or 10 μM 25-HC for the indicated hours before proteins were extracted for Western blotting to detect the E-cadherin, Snail, N-cadherin and Vimentin expressions. (B) LoVo cells were stimulated with 10 μM 25-HC for 24 hours and cells were collected for immunofluorescent staining to determine the E-cadherin, N-cadherin and Vimentin expressions. (C) The mRNA (C) and protein (D) expression of E-cadherin, N-cadherin and Vimentin in xenografts from the nude mice were detected by RT-qPCR and Western blotting, respectively. Results were obtained from 3 independent experiments and are expressed as the means ± SEM. *p<0.05, **p<0.01.

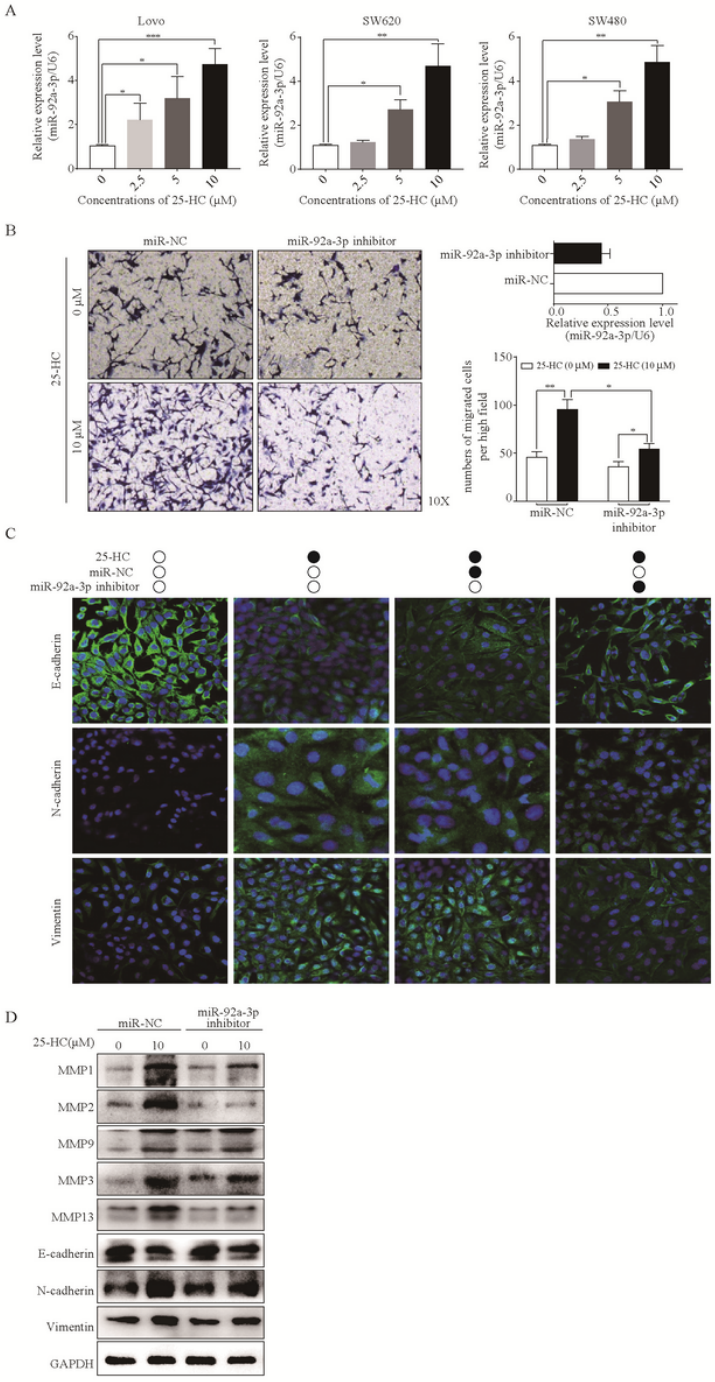

Figure 5

Inhibition of miR-92a-3p decreases 25-HC-induced cells migration by regulating EMT in CRC cells. (A) LoVo, SW620 and SW480 cells were treated with 25-HC for 24 hours, the expression of miR-92a-3p was detected by RT-qPCR. LoVo cells were transfected with miR-92a-3p inhibitor or its negative control (NC) for 24 hours before treated with 25-HC for 24 hours, (B) cells were collected for RT-qPCR to detect the miR-92a-3p expression or cells migration was determined by Transwell assay. Results were obtained from 3 independent experiments. (C) Immunofluorescent staining to determine the E-cadherin, N-cadherin and Vimentin expressions. Results were obtained from 2 independent experiments. (D) The protein level of of E-cadherin, N-cadherin and Vimentin were detected by Western blotting. Results were obtained from 3 independent experiments and are expressed as the means ± SEM. *p<0.05, **p<0.01, ***p< 0.001.

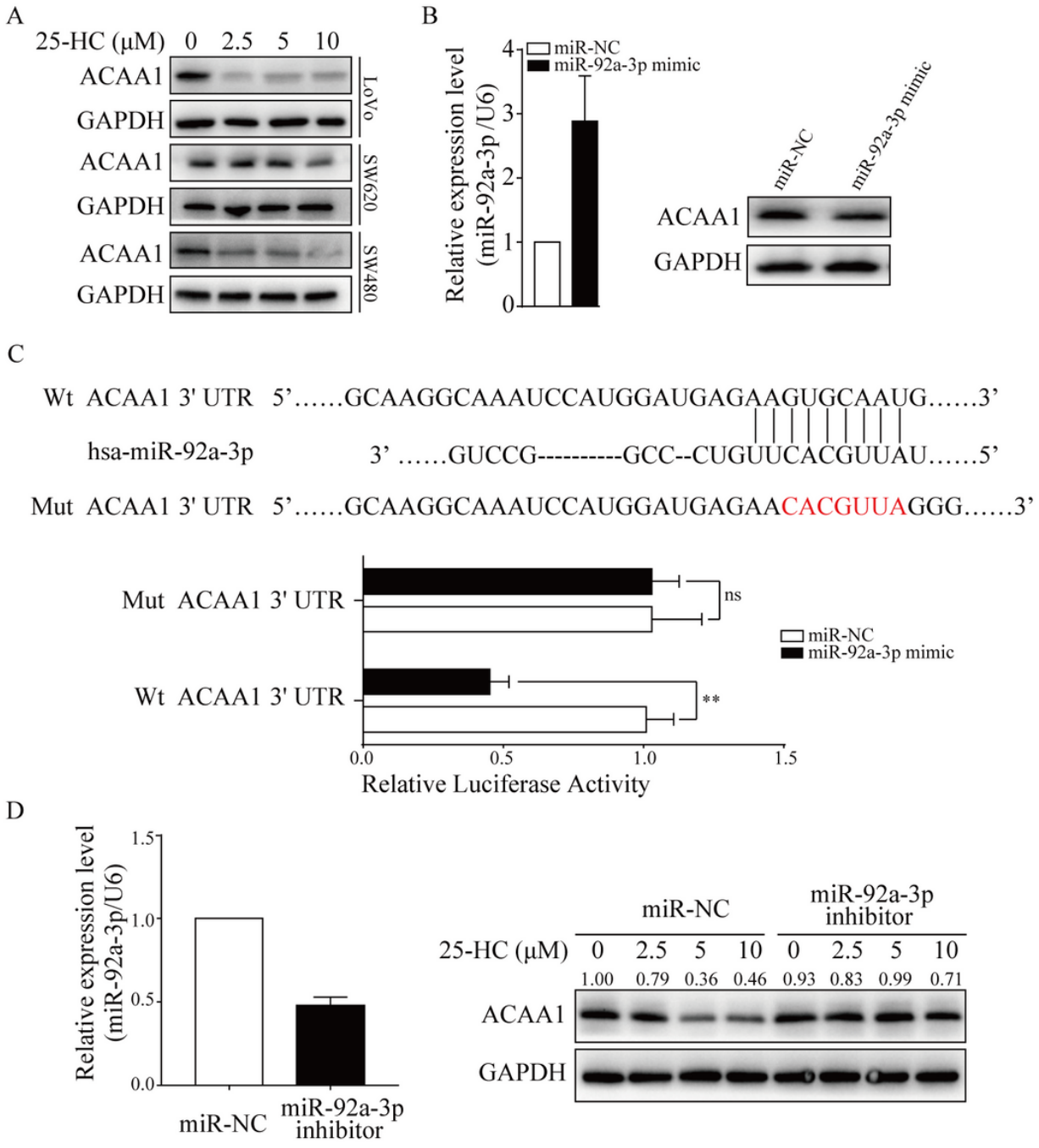

Figure 6

ACAA1 is a direct target of miR-92a-3p. (A) LoVo, SW480 and SW620 cells were stimulated with 25-HC for 24 hours and the protein level of ACAA1 was analyzed by Western blotting. (B) MiR-92a-3p mimic or its negative control (miR-NC) was transfected into LoVo cells for 48 hours, the miR-92a-3p expression was determined by RT-qPCR and the ACAA1 expression was analyzed by Western blotting. (C) TargetScan predicted the miR-92a-3p binding sites in the ACAA1 3'-UTR. The sites targeted by mutagenesis are indicated. LoVo cells were co-transfected with miR-92a-3p and Wt ACAA1-3'-UTR or Mut ACAA1-3'-UTR for 48 hours, and cells were collected for dual luciferase reporter assay. (D) LoVo cells were transfected with miR-92a-3p inhibitor or its negative control (miR-NC) for 24 hours, and cells were collected for RT-qPCR or cells were treated with the indicated concentrations of 25-HC for 24 hours before the

expression of ACAA1 was analyzed by Western blotting. Results were obtained from 3 independent experiments and are expressed as the means ± SEM. **p<0.01, ns: not significant.

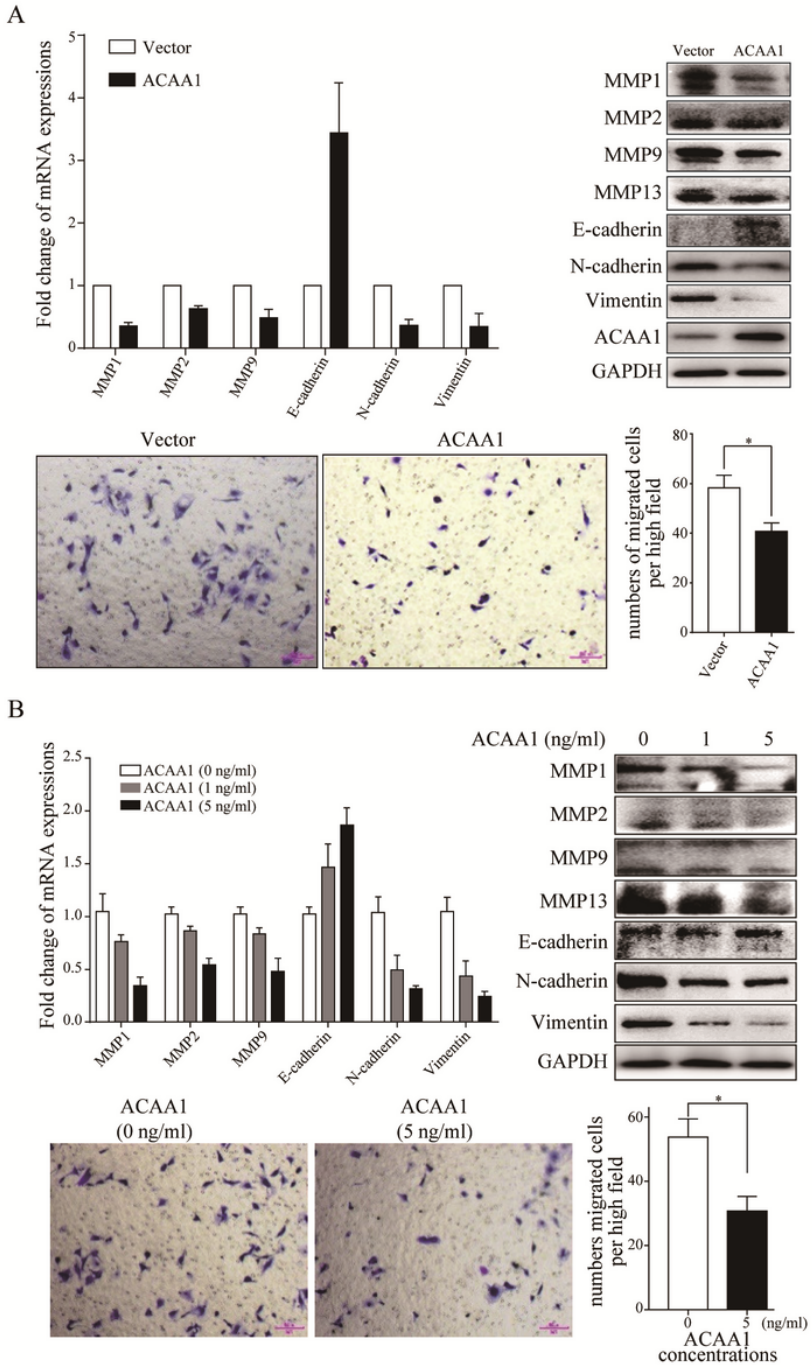

Figure 7

ACAA1 inhibits CRC cells migration. LoVo cells were transfected with ACAA1 plasmid or control vector for 24 hours (A) or stimulated with ACAA1 for 24 hours (B). Cells were collected for RNA or protein extraction to determine the MMP1, MMP2, MMP9, E-cadherin, N-cadherin and Vimentin expressions by RT-qPCR or Western blotting or cells migration was performed by Transwell assay. Results were obtained from 3 independent experiments and are expressed as the means ± SEM. *p<0.05.

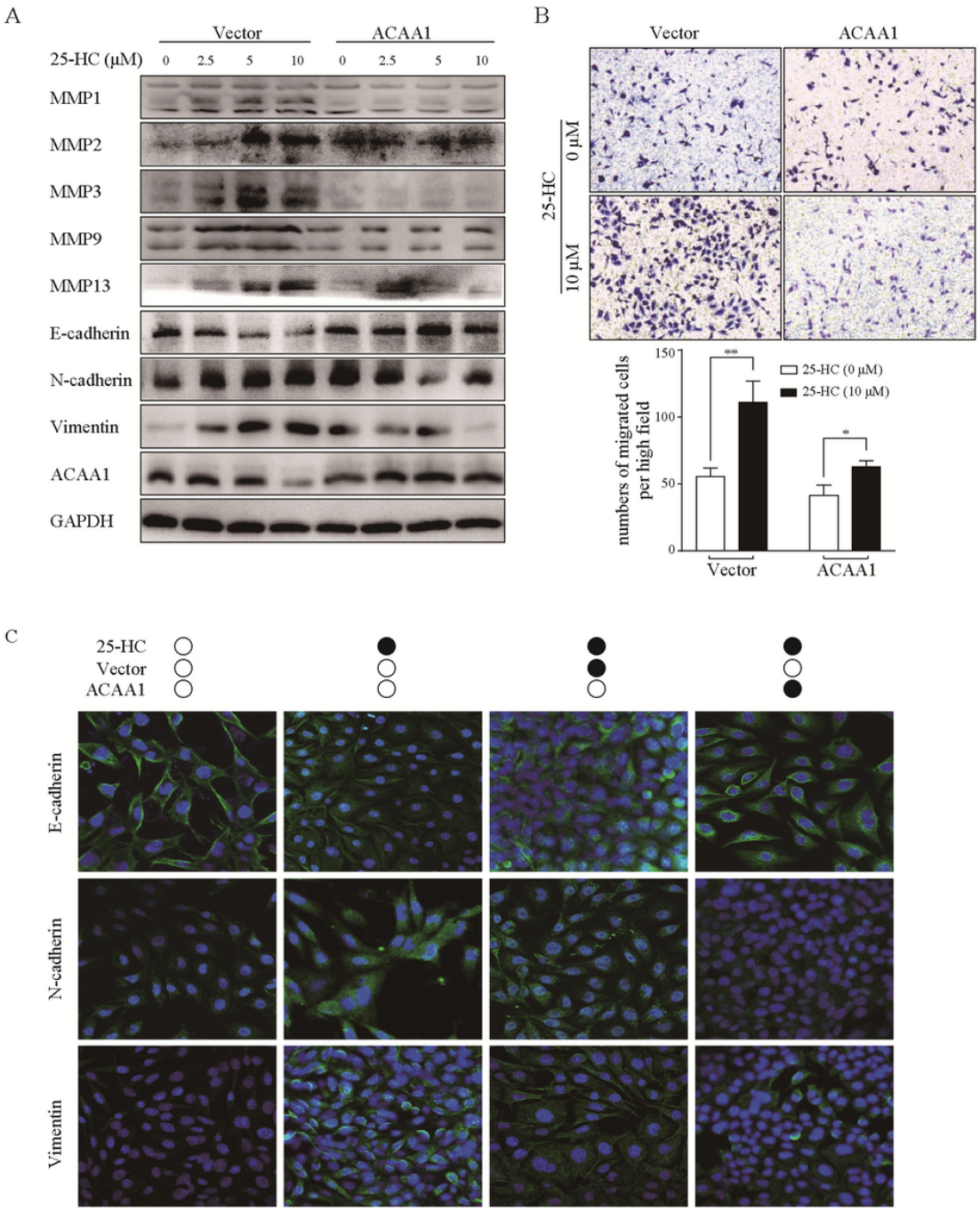

Figure 8

Over-expression of ACAA1 decreases 25-HC-induced cells migration by regulating EMT in CRC cells. (A) LoVo cells were transfected with ACAA1 plasmid or control vector for 24 hours before treated with the indicated concentrations of 25-HC. 24 hours later, (A) Cells were collected for protein extraction to determine the MMP1, MMP2, MMP3, MMP9, MMP13, E-cadherin, N-cadherin and Vimentin expressions by Western blotting. (B) Cells migration was performed by Transwell assay. (C) LoVo cells were transfected with ACAA1 plasmid or control vector for 24 hours before treated with the 10 μM 25-HC. 24 hours later, cells were collected for immunofluorescent staining to determine the E-cadherin, N-cadherin and Vimentin expressions. Results were obtained from 3 independent experiments and are expressed as the means ± SEM. *p<0.05, **p<0.01.

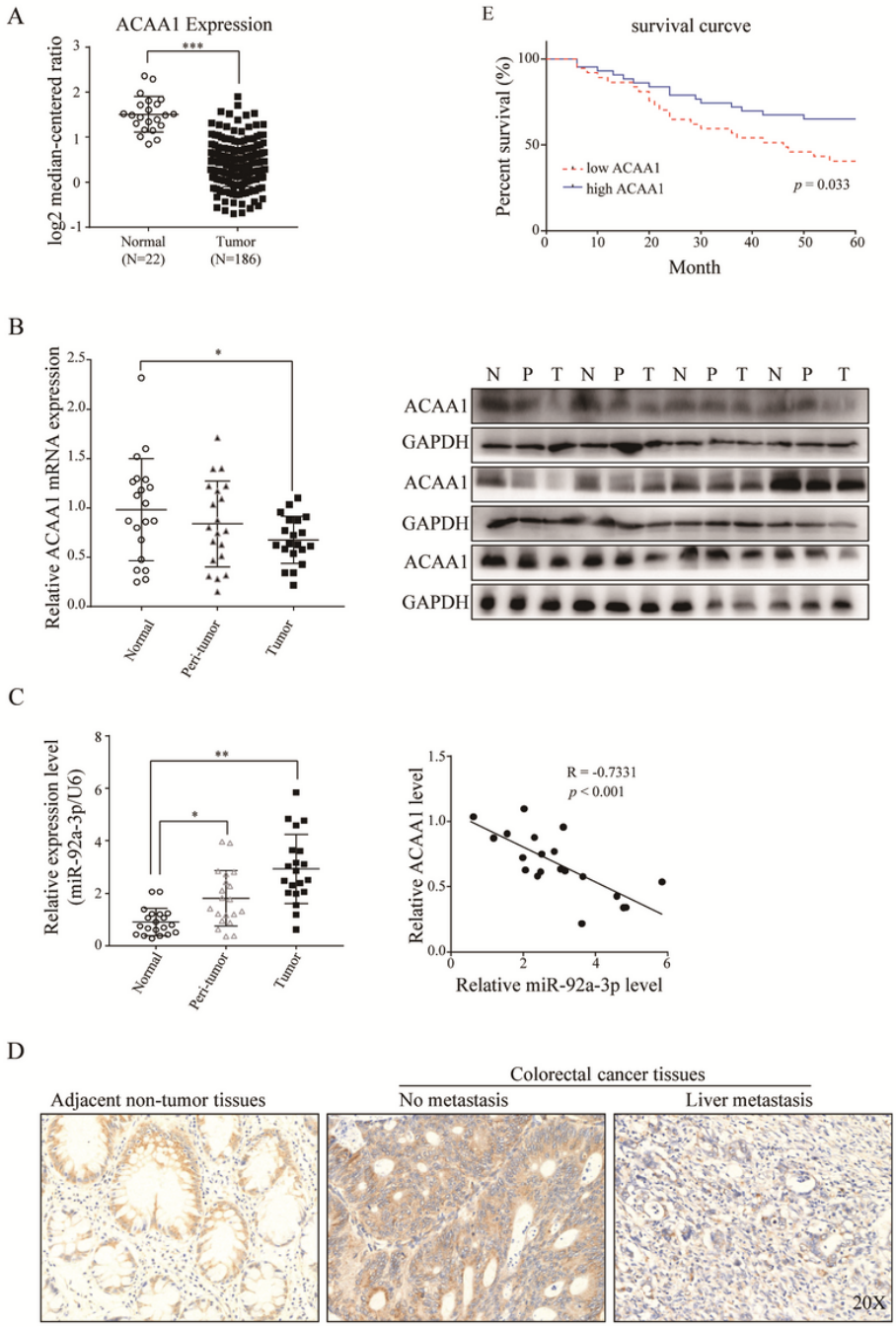

Figure 9

ACAA1 is down-regulated in CRC and is associated with a good prognosis in CRC patients. (A) Bioinformatics analysis of ACAA1 expression in CRC tumors and normal tissues from TCGA database. (B) The expressions of ACAA1 in 20 CRC tumor, peri-tumor and normal tissues were determined by RT-qPCR or Western blotting, respectively. (C) The expression of miR-92a-3p in 20 CRC tumor, peri-tumor and normal tissues was determined by RT-qPCR and its expression relationship with ACAA1 was analyzed. (D) IHC analysis of ACAA1 expression in 80 CRC samples. Representative images are shown. (E) Overall survival analysis of CRC patients with ACAA1 expression in 80 samples. Data are expressed as the means ± SEM. *p<0.05, **p<0.01, ***p<0.001.

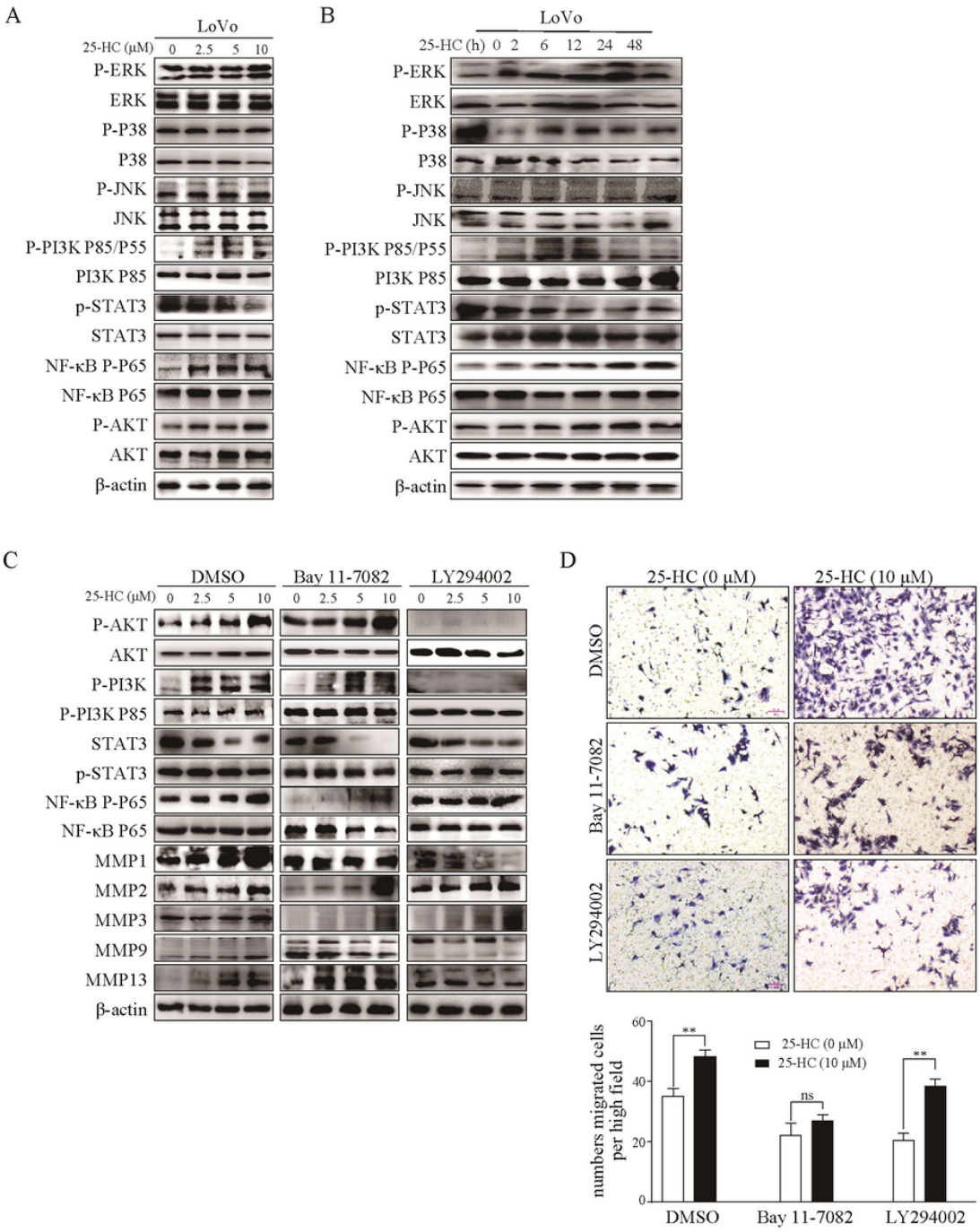

Figure 10

Inhibition of NF-κB signaling decreases 25-HC-induced cells migration. LoVo cells were treated with the indicated concentrations of 25-HC for 24 hours (A) or 10 μM 25-HC for the indicated hours (B) before cells were collected for protein extraction to determine the activation of related signaling pathways by Western blotting. LoVo cells were pre-treated with Bay 11-7082 or LY294002 for 2 hours before treated with the indicated concentrations of 25-HC for 24 hours, (C) Cells were collected for protein extraction to determine the activation of related signaling pathways by Western blotting. (D) Cells migration was performed by Transwell assay. Results were obtained from 3 independent experiments and are expressed as the means ± SEM. **p<0.01, ns: not significant.

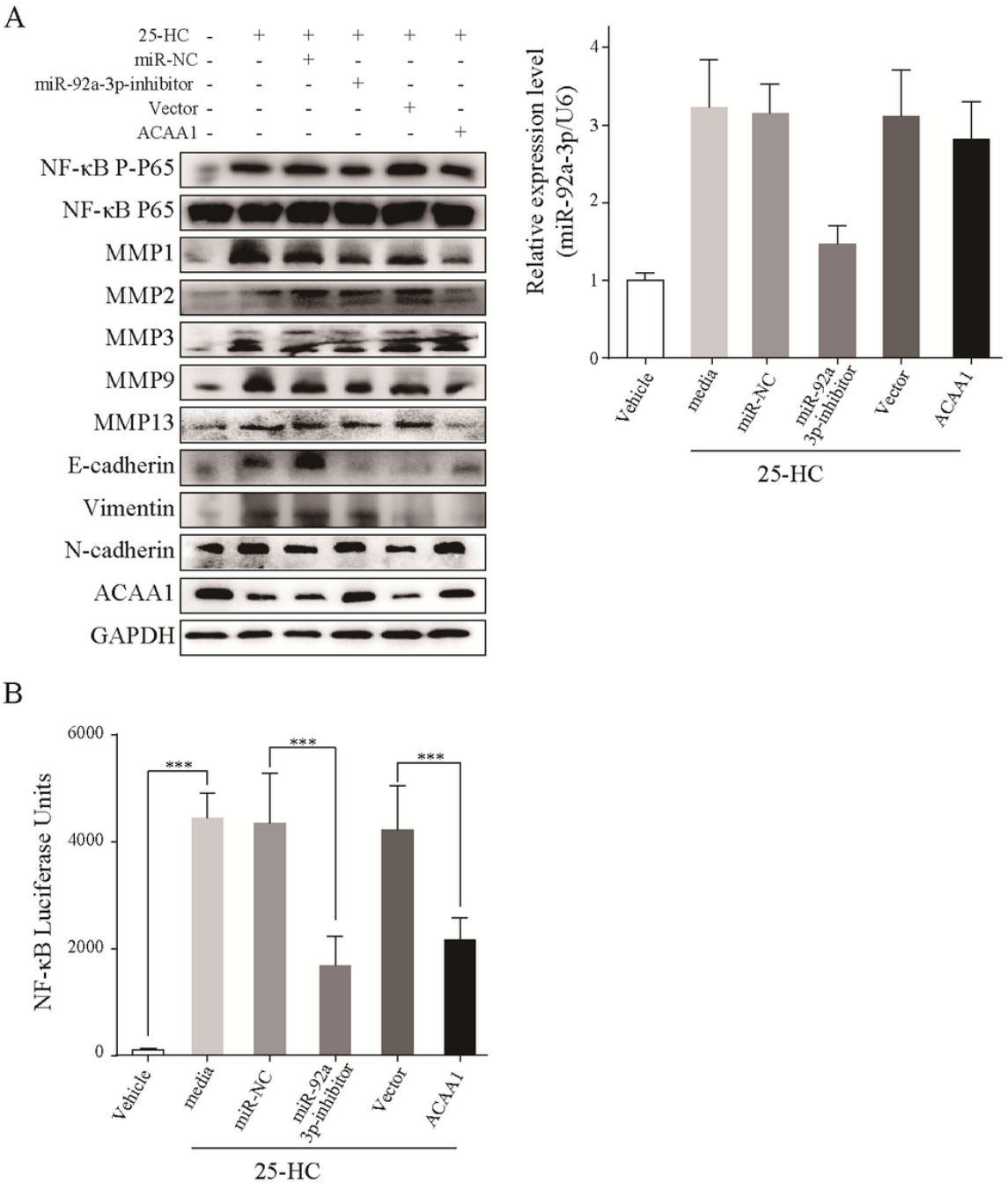

Figure 11

Inhibition of miR-92a-3p or over-expression of ACAA1 inhibits the NF-κB activation induced by 25-HC. (A) LoVo cells were transfected with ACAA1 plasmid or miR-92a-3p inhibitor or its control vectors for 24 hours before treated with 10 μM 25-HC. 24 hours later, cells were collected for protein or RNA extraction to determine the NF-κB P-P65, MMP1, MMP2, MMP3, MMP9, MMP13, E-cadherin, N-cadherin and Vimentin expressions by Western blotting or miR-92a-3p expression by RT-qPCR, respectively. (B) NF-κB luciferase reporter plasmid was co-transfected into LoVo cells with ACAA1 plasmid or miR-92a-3p inhibitor or its control vectors for 24 hours before treated with 10 μM 25-HC. 24 hours later, cells were collected and the luciferase activities were determined. Results were obtained from 3 independent experiments and are expressed as the means ± SEM. ***p<0.001.